A theory for time correlation functions in liquids

Jianshu Cao and Gregory A. Voth
Department of Chemistry, University of Pennsylvania, Philadelphia, Pennsylvania 19104-6323

(Received 27 January 1995; accepted 1 June 1995)

A theory for time correlation functions in liquids is developed based on the optimized quadratic approximation for liquid state potential energy functions. The latter approximation leads to the rigorous mathematical definition of inherent structures in liquids and their vibrational fluctuations, in turn leading to the concept of inherent normal modes in the liquid state. These normal modes are called ''optimized normal modes.'' Unlike normal modes based on instantaneous liquid state configurations, the optimized normal modes are stable, having real-valued frequencies, and each inherent liquid state structure has a different set of modes associated with it. By including a single phenomenological decay function which captures the average transition rate between the different sets of normal modes, velocity time correlation functions and dynamical friction kernels for solute bonds can be predicted in good agreement with direct molecular dynamics simulation results. © *1995 American Institute of Physics.*

I. INTRODUCTION

One of the basic ingredients in condensed matter theory[1,2] is the concept of phonons, i.e., the small oscillations about a stable structure or the energy minimum, which can be related to many equilibrium and transport properties such as heat capacity, thermal conductivity, thermal expansion, light scattering, etc. It is clear, however, that liquids are different from solids because of their lack of stable structures, making it formally difficult to apply the well-developed theory of phonons in order to calculate, e.g., time correlation functions and thereby predict experimental observables. A clear challenge, therefore, is to derive from first principles a set of ''modes'' which to some degree dominate the molecular motions in liquids, at least for times smaller than some phenomenological relaxation time of such modes.[3,4] The purpose of this paper is to provide a formal prescription for defining such modes which we call ''optimized normal modes'' (ONM). A related and challenging problem is the microscopic origin of the relaxation behavior of these modes, but this issue will be left to future research.

It should be noted that the theory described herein builds on the earlier work of Stillinger and Weber[5–7] and of Zwanzig.[8] The former authors proposed the inherent structure picture of liquids in which such structures are determined by a steepest-decent quench on the liquid state potential hypersurface. The many-body phase space is thus divided into subspaces corresponding to many different local minima. The distribution of the inherent structure local minima depends on the interaction potential, temperature, and density. The Stillinger and Weber stable states,[5–7] being local potential minima, are free of imaginary frequencies and thus ideal candidates for an effective harmonic approximation. Unlike in solids, however, the inherent structure is a metastable state so there must be an overall decay behavior associated with the transitions between the metastable states. Though rich in physical insight, the work by Stillinger and Weber did not provide a variational procedure for defining the inherent structures and their associated vibrational modes for a given set of thermodynamical state variables (e.g., temperature).

In his dynamical view of liquids, Zwanzig[8] suggested that after some of vibrational motion about an inherent structure minimum, the liquid will jump through a saddle point to another local minimum and its associated vibrations. Eventually, the liquid will explore all the phase space available to it. The transition process is characterized by an average lifetime ''τ'' and thus an exponential decay factor is imposed on the harmonic motion. The identification of the inherent structures, the vibrational motion about them, and the interminima transitions provides a plausible picture of the underlying dynamical behavior of a liquid. Based on this picture, Zwanzig[8] derived an expression for the self-diffusion constant and a relation between self-diffusion and viscosity which is consistent with the Stokes–Einstein law. In this theory, Zwanzig invoked the idea of inherent structure modes, but he did not explicitly define those modes starting with the microscopic potential (i.e., he used a Debye-like approximation). In the present paper, a mathematical procedure is used to specify the inherent structure modes (i.e., the optimized normal modes) which provides the missing element in Zwanzig's picture. (See also Refs. 9 and 10 for another such approach.)

In our previous study on the formulation of statistical mechanics based on an effective quadratic potential,[11] the exact cumulant expansion of the partition function was shown to have a one-to-one correspondence with a diagrammatic representation. It was also shown that diagrammatic classifications and topological reductions result in the renormalization of the three diagrammatic elements and thus lead to a set of self-consistent effective quadratic equations at different levels of approximation. The theory is applicable to both classical and quantum systems, and can be shown in the extremely low temperature limit to be equivalent to ground state calculations in a harmonic oscillator basis set. Among the central results of the formalism[11] is the optimized quadratic approximation (OQA) for the partition function which is of special importance because of its applicability to realistic many-body systems. The lowest-order OQA equations

can be derived from the diagrammatic approach or, equivalently, from the Gibbs–Bogoliubov variational principle. It can be shown that the optimized quadratic reference potential represents the best fit to an anharmonic potential and any further corrections are beyond the effective potential description.

Similar to the inherent structure picture, there exist multiple solutions to the OQA equations at different positions, each corresponding to a local potential minimum with its associated effective normal mode frequencies. Therefore, the OQA solutions separate the many-body potential hypersurface into different regions, each having a definite thermal partition, and all physical quantities can be expressed as a superposition of the OQA expectation values weighted by the thermal partitions. The nature of the OQA solution on a many-body hypersurface reveals the distinction between solids, liquids, and glasses, as well as the transitions between those phases. When applied to liquids, this theory defines the inherent structures within a rigorous theoretical framework and, furthermore, introduces the optimized normal modes (ONM) of oscillation in a well-defined fashion. Thus, to a reasonable degree of mathematical rigor, there exist solid statelike concepts in liquids such as equilibrium structures and phonon excitations, though they are of a metastable nature.

The notion of inherent structures and their optimized normal modes immediately induces one to extend the OQA theory to characterize the dynamics of liquid state systems, particularly time correlation functions. At the level of the OQA, the approach expresses the time correlation function as a thermal partition-weighted superposition of optimized harmonic oscillator time correlation functions. As suggested by Zwanzig,[8] such a linear description is adequate for a time interval shorter than some relaxation time, beyond which the effective harmonic motion for an inherent structure decays into the effective harmonic motion for a different inherent structure. Motivated by this physical intuition, a decay factor is incorporated into the expression for the time correlation function predicted by the optimized normal modes, thus introducing a broadening of the spectrum which defines damped normal modes (DNM). The decay function describes the average long time decay of correlations due to the transitions between the normal modes of different inherent structures. It will be shown that the combination of the DNM picture with the self-consistent OQA proves to be a fruitful theoretical framework for predicting liquid state time correlation functions.

Another outgrowth of the present theory applies to a wide variety of processes involving intramolecular motions in liquids which can be modeled by the generalized Langevin equation (GLE).[3,12,13] In the GLE approach, the dynamical solvent effect on, e.g., a molecular bond or some more complicated solute coordinate is characterized by a dynamic friction kernel which can be predicted theoretically only in the simple case of translational and rotational motions.[14,15] Though the validity of the GLE has not been proven in general, it can be rigorously derived for a Gaussian bath which consists of harmonic oscillators linearly coupled to the solute.[4] It will be shown that the OQA and DNM theory can be extended to identify the bath normal modes in a many-body system and their coupling coefficients to a solute, thus providing a theory for the friction kernel in the GLE picture. This generalization of the theory has important implications for the study of friction on solute bond vibrations as well as activated barrier crossing. In accord with the Zwanzig picture, the GLE bath from the DNM theory experiences an exponential decay because of the transitions between different inherent structure OQA solutions. By assuming that the exponential decay parameter can be determined from the self-diffusion behavior of the *pure solvent*, one can predict the dynamical friction kernel for a *solute* bond in good agreement with the exact result from MD simulations.[16] We believe this result to be significant because, in principle, it provides a microscopic theory for the GLE friction kernel in liquids.

Before proceeding to the next section, it is important to contrast the present theory with the concept of ''instantaneous normal modes'' (INM).[9,10,17–25] In the latter theory, the liquid state potential is Taylor expanded at different instantaneous configurations through quadratic order. A set of normal modes is then obtained by diagonalizing the force constant matrix and the short time dynamics resulting from that liquid configuration can be predicted. This effective harmonic motion is suggested to persist up to some characteristic relaxation time, at which point it is transformed into motion characteristic of another set of instantaneous normal modes.[9,10,17–25] The overall short time dynamics of the liquid is thereby determined by a superposition of the harmonic motions of all possible configurations. The liquid state ''phonon spectrum'' is taken to be the ensemble average of the instantaneous normal modes of the liquid configurations.[17] Instantaneous normal modes have been used to study, e.g., the short-time dynamics of coupled translational and rotational motions in molecular fluids.[19] The predictions of the short-time harmonic motion were compared with exact molecular dynamics (MD) simulation results and found to agree only for short times. As a result of the anharmonicity in the liquid, the difficulty in describing such correlation functions with the INM theory arises due to the presence of the unstable modes which diverge exponentially with time. From this point of view, it is mainly the unstable modes which destroy the linear motion of the liquid. Since the imaginary frequencies presumably become operational after the characteristic relaxation time, it can be argued that the unstable modes should be removed from the INM correlation function.[19,20] Reasonable agreement with exact MD correlation functions can be obtained when this ''stable mode'' approximation is implemented.[19,20,26,27] The underlying ONM spectrum in the DNM theory does not contain globally unstable modes, and it involves a rather different set of assumptions and approximations in its formulation. The predictions of the stable mode INM and DNM theories will be compared numerically for several examples in Sec. IV.

The sections of this paper are organized are follows: In Sec. II, the DNM analysis of inherent structures is presented within the rigorous OQA framework. Then, in Sec. III the GLE picture is formulated in terms of constrained OQA equations and the DNM theory. Some illustrative numerical

examples are presented in Sec. IV and concluding remarks are given in Sec. V.

II. DAMPED NORMAL MODE THEORY OF LIQUIDS

In an effort to bring conceptual order to the disordered liquid state, Stillinger and Weber[5–7] advanced the idea of separating the statistical mechanical description of liquids into two distinct parts, namely, the mechanically stable packing part and the thermally fluctuating part. Their key idea was a configurational mapping where arbitrary sets of molecular positions are referred to potential minima which are the *inherent structures* underlying the liquid phase. This mapping is generated by a quench procedure which follows the steepest-descent paths on the hypersurface of the many-body system. Much attention has been focused on the identification and characterization of these mechanically stable packings.

The formalism of Stillinger and Weber[5] begins with the canonical partition function for N structureless classical particles, given by

$$Z_N = \int d\mathbf{q}\, \exp[-\beta V(\mathbf{q})], \tag{2.1}$$

where N is the particle number and the usual normalization factor is omitted here for simplicity. The configurational integral is next broken into the separate contributions from each quench region, i.e.,

$$Z_N = \sum_l \int_{R(l)} d\mathbf{q}\, \exp[-\beta V(\mathbf{q})], \tag{2.2}$$

where $R(l)$ defines the segment on the potential hypersurface which can be uniquely mapped to the inherent structure designated by the index l. Within the region $R(l)$, any set of coordinates can be traced to the quenched inherent structure, giving

$$V(\mathbf{q}) = V(\mathbf{q}_l) + \Delta_l V(\mathbf{q}), \tag{2.3}$$

where $V(\mathbf{q}_l)$ is the potential local minimum, satisfying

$$\boldsymbol{\nabla} V(\mathbf{q}_l) = 0, \tag{2.4}$$

and $\boldsymbol{\nabla}$ denotes the spatial derivative. Consequently, the partition function can be rewritten as

$$Z_N = \sum_l \exp[-\beta V(\mathbf{q}_l)] \int_{R(l)} d\mathbf{q}\, \exp[-\beta \Delta_l V(\mathbf{q})], \tag{2.5}$$

where the integration accounts for the thermal fluctuations around the stable packing structure.

While the quench procedure may reveal the *hidden structures* of the liquid phase, it may not be particularly successful in recovering the equilibrium properties of liquids and even less successful in predicting their dynamical properties. While the thermal fluctuations in the inherent structure potential wells are suggestive of a linear harmonic motion, it turns out that thermally broadening the quenched structure by using an Einstein or Debye vibrational approximation fails to reconstruct important features such as pair correlation functions. There are at least two reasons for this, one being the significant anharmonicities of the liquid state interaction potential and the other being the geometric disorder of the inherent structures. Thereby, an actual set of effective harmonic modes will bear little resemblance to the phonon spectrum of solids as described by the Einstein or Debye models. Evidently, a systematic theory is required to formalize the concept of inherent structures, to establish the relationship between liquid dynamics and collective harmonic motions, and to allow for higher-order corrections. This goal can be accomplished within the framework of the OQA theory developed for general potentials in Ref. 11.

To start, the OQA of Ref. 11 for an N-body coordinate space is briefly reviewed. Here, vectors and matrices are denoted by bold fonts, and optimized frequencies and positions are denoted by bars. The basic OQA equations can be written as

$$\langle \boldsymbol{\nabla} V(\overline{\mathbf{q}} + \tilde{\mathbf{q}}) \rangle_{\mathbf{C}} = 0, \tag{2.6}$$

$$\langle \boldsymbol{\nabla} : \boldsymbol{\nabla} V(\overline{\mathbf{q}} + \tilde{\mathbf{q}}) \rangle_{\mathbf{C}} = \mathbf{K}, \tag{2.7}$$

where $\mathbf{K}$ is the optimized effective force constant matrix and $\boldsymbol{\nabla}$ is the partial derivative vector $\boldsymbol{\nabla}_i = \partial/\partial_i$. The notation $\langle \cdots \rangle_{\mathbf{C}}$ here denotes a multidimensional Gaussian average centered at $\overline{\mathbf{q}}$, i.e.,

$$\langle V(\overline{\mathbf{q}} + \tilde{\mathbf{q}}) \rangle_{\mathbf{C}} = \frac{1}{\sqrt{\det[2\pi \mathbf{C}]}} \int d\tilde{\mathbf{q}}\; V(\overline{\mathbf{q}} + \tilde{\mathbf{q}}) \times \exp[-\tilde{\mathbf{q}} \cdot \mathbf{C}^{-1} \cdot \tilde{\mathbf{q}}/2], \tag{2.8}$$

where the Gaussian width factor matrix $\mathbf{C}$ is formally expressed in the classical limit as

$$\mathbf{C} = (\beta \mathbf{K})^{-1}. \tag{2.9}$$

In terms of the eigensolutions, a unitary matrix $\mathbf{U}$ can be found to diagonalize the mass-scaled force constant matrix $\mathbf{K}$, giving the effective normal modes, i.e.,

$$\mathbf{U}^{\dagger} \overline{\mathbf{K}} \mathbf{U} = [\mathbf{I} \cdot \overline{\omega}^2], \tag{2.10}$$

where $\{\overline{\omega}\}$ is the set of the eigenfrequencies, $\mathbf{I}$ is the $3N$-dimensional identity matrix, and $[\mathbf{I} \cdot \overline{\omega}^2]$ denotes a diagonal matrix with the ith diagonal element given by $\overline{\omega}_i^2$. The Gaussian width factor matrix in Eq. (2.9) can also be determined from the relation

$$\mathbf{C} = \overline{\mathbf{U}} [\mathbf{I} \cdot \overline{\alpha}] \overline{\mathbf{U}}^{\dagger}, \tag{2.11}$$

where $\overline{\mathbf{U}} = \mathbf{m}^{-1/2} \mathbf{U}$, $\mathbf{m}$ is the diagonal mass matrix, and the individual elements of the normal mode mass-scaled thermal width vector are given in the classical limit by

$$\overline{\alpha}_i = 1/\beta \overline{\omega}_i^2. \tag{2.12}$$

Thus, the set of optimized frequencies $\{\overline{\omega}\}$ and average positions $\{\overline{q}\}$ are variationally obtained as the self-consistent solution to the transcendental matrix equations Eqs. (2.6) and (2.7) in N-dimensional space. The quantum generalization of the OQA equations is given in the Appendix.

As it stands, there are many possible solutions to the self-consistent OQA equations, each being defined in a local potential well of the many-body system. Under the condition that different wells are separated, i.e., the barrier between any two neighboring wells is significantly higher than the

average thermal energy, one can assume a linear superposition of all the metastable solutions. In this spirit, the partition function in Eq. (2.1) is intrinsically separated into different integration regions and can be written in the quadratic approximation as[11]

$$Z_N \simeq \sum_l Z_{l,\mathrm{ref}} \exp[-\beta\langle \Delta V(\overline{\mathbf{q}}_l+\tilde{\mathbf{q}})\rangle_{\mathbf{C}_l}], \tag{2.13}$$

where subscript l denotes the lth set of OQA solutions to Eqs. (2.6) and (2.7). In this sense, the differences between liquids and solids can be attributed to the nature of the OQA solutions for the many-body configurations. Indeed, this important concept makes it possible to rigorously represent the inherent structures for liquids, which was previously proposed and pursued from the perspective of quenched potential minima, and to introduce an optimized normal mode spectrum which will be an analog to the phonon spectrum of solids.[1,2] To be more explicit, one can identify $\overline{\mathbf{q}}$, i.e., the solution to Eq. (2.6), as the inherent structures, and the corresponding eigenvectors and eigenvalues, i.e., the solution to Eq. (2.7), as the optimized normal modes (ONM) for the inherent structure. This definition differs significantly from that of Stillinger and Weber's quenched minima for it incorporates the packing structures and thermal fluctuations into a unified theory. The equilibrium state of the inherent structure defined in the OQA will shift from the mechanical equilibrium state because of the thermal motion, while the distribution of the optimized normal modes will display very different features from the Einstein or Debye model which are only meaningful for well-defined solid lattices. Moreover, the formulation here is applicable to both classical and quantum Boltzmann liquids (cf. the Appendix). Along these lines, we note that the mechanical equilibrium state in Stillinger and Weber's theory lacks a plausible interpretation in quantum mechanics because inherent quantum fluctuations must introduce uncertainties in the particle positions.

In general, all expectation values of physical variables can be expressed as the sum of the distinct OQA solutions weighted by the partitions of the metastable wells. To take into account the weight of each solution correctly, the mapping method, introduced as the main ingredient in Stillinger and Weber's approach, proves to be helpful. In this approach, the liquid hypersurface is divided into regions $R(l)$, each of which can be mapped uniquely to an OQA inherent structure. Correspondingly, certain instantaneous liquid configurations are traced to the same OQA solution, while other OQA inherent structures must correspond to different subsurfaces on the liquid potential hypersurface. In practice, a mapping procedure can be devised as follows:

(a) Randomly select an instantaneous liquid configuration from the canonical distribution;
(b) quench the liquid configuration to its potential minimum;
(c) solve the self-consistent optimized quadratic approximation near the mechanical stable structure;
(d) collect data for the optimized inherent structure;
(e) repeat steps (a)–(d) for many independent liquid configurations.

Because of the one-to-one correspondence of the mapping, the thermal partition of the optimized quadratic solutions is accurately incorporated into the scheme. The quench in the procedure can be achieved by the steepest-descent or the conjugated gradient algorithms. Many physical properties can be investigated within the frame of the optimized quadratic theory. In particular, the transition between the solid and the liquid states can be viewed as the change from a global inherent structure to many possible metastable structures. This paper, however, is devoted to the study of liquid state *dynamics* based on this model.

To begin the dynamical analysis, one can define an ONM spectrum such that

$$D_{\mathrm{ONM}}(\omega) = \frac{1}{3N}\sum_{i=1}^{3N} \langle \delta[\omega - \overline{\omega_i}(\mathbf{q}_0)]\rangle_{\mathbf{q}_0}, \tag{2.14}$$

where $\overline{\omega_i}(\mathbf{q}_0)$ are the set of eigensolutions to Eq. (2.10) for the region $R(l)$ mapped from an instantaneous liquid configuration $\mathbf{q}_0$. The average in Eq. (2.14) is from the canonical distribution of instantaneous liquid configurations. The optimized normal modes variationally capture the characteristic stable mode thermal excitations,[11] at least for the time period when the system remains in the metastable potential well. In contrast, the INM description[9,10,17–25] is instantaneous by nature and, through the continuity of the fluid motion, renders instabilities to some of the modes. The ONM spectrum is essentially the liquid state analog of the self-consistent phonon spectrum of anharmonic solids.[28–30]

On the other hand, the metastability of the optimized normal modes tends to destroy the coherence of their vibrations. The liquid motion can be viewed as transitions from one optimized inherent structure to another, an interplay of barrier crossings and thermal vibrations. The short lifetime of the ONM's will broaden the overall spectrum as in the case of a damped oscillator. This dynamical picture is included by introducing a decay factor into the time correlation functions. For example, the velocity time correlation function for a simple atomic fluid may be written as

$$C_{\mathrm{DNM}}(t) = \frac{1}{m\beta}\int d\omega\, D_{\mathrm{ONM}}(\omega)\cos(\omega t) f(\omega,t), \tag{2.15}$$

where the subscript DNM stands for the "damped normal mode" approximation and $f(\omega,t)$ is a decay function which may, in the most general case, depend on the frequency. A simplifying assumption here is to adopt a simple monotonic decay function which ignores the frequency dependence such that the DNM spectrum now reads

$$D_{\mathrm{DNM}}(\omega) = \int d\omega'\, F(\omega-\omega') D_{\mathrm{ONM}}(\omega'), \tag{2.16}$$

where $F(\omega)$ is the Fourier transform of the universal decay function which broadens the ONM spectrum.

Since a procedure to determine the functional form of the decay function from first principles has not yet been developed, it can simply be assumed to be an exponential function, i.e.,

$$f(t) = \exp(-\lambda|t|) \tag{2.17}$$

with the corresponding spectral convolution function $F(\omega)$ given by

$$F(\omega)=\frac{1}{\pi}\frac{\lambda}{\lambda^2+\omega^2} \tag{2.18}$$

which takes the form of a Lorentzian broadening function. Since $f(t)$ is not an analytic function at $t=0$, the decay constant λ cannot be determined from the short time behavior of a time correlation function. From the microscopic point of view, λ can be understood as the average escape rate from the OQA inherent structures. Therefore, one might estimate this constant from transition state theory (TST)[13,31] provided the typical values of the ONM frequencies and the barrier heights are available. Alternatively, we note that Eq. (2.16) with the Lorentzian broadening factor Eq. (2.18) is exactly the expression introduced by Zwanzig in his analysis of the self-diffusion constant.[8] In the context of the present DNM theory, one can therefore adjust the decay constant λ to yield the correct *experimental* diffusion constant, i.e.,

$$D=\int d\omega\ \frac{1}{\pi}\frac{\lambda}{\lambda^2+\omega^2}\,D_{\mathrm{ONM}}(\omega), \tag{2.19}$$

which is the zero-frequency component of the Fourier transform of the velocity autocorrelation function. With the quantities $D_{\mathrm{ONM}}(\omega)$ and λ in hand, other liquid state correlation functions can then be predicted (cf. the next section). A similar approach has been proposed in Ref. 10 in order to introduce damping into the stable mode INM theory.

Before proceeding to the applications of the theory, we note that an alternative choice of $f(t)$ is a Gaussian decay function, i.e.,

$$f(t)=\exp(-\kappa t^2/2), \tag{2.20}$$

where κ is an undetermined constant, and the spectral convolution function is given in this case by

$$F(\omega)=\sqrt{\frac{\kappa}{2\pi}}\exp(-\omega^2/2\kappa) \tag{2.21}$$

which broadens a single frequency into a Gaussian distribution with a width factor κ. The Gaussian choice of damping function $f(t)$ allows one to impose the condition

$$\omega_e^2=\int d\omega\ D_{\mathrm{ONM}}(\omega)\omega^2+\kappa, \tag{2.22}$$

where ω_e is the ''Einstein frequency'' calculated from equilibrium properties via the second-order moment expansion. This approach uniquely specifies the Gaussian width factor κ. The optimal choice of the damping function $f(t)$ will depend on the problem at hand and the time scale of the behavior under examination. The two choices described here are, of course, qualitatively different since one (the Gaussian) is based on short time (inertial) behavior, while the other (the exponential) is based on longer time (diffusive) behavior. In the examples studied in Sec. IV B, an exponential damping function was found to be superior, but this is not necessarily always true.

III. DYNAMICAL FRICTION ON SOLUTE BONDS

The generalized Langevin equation (GLE) has been used to understand a wide range of problems involving molecular motion in liquids such as activated barrier crossing and vibrational relaxation.[3,4,12,13] The GLE for a molecular bond can be expressed as

$$m\ddot{q}(t)+m\tilde{\omega}^2q(t)+\int_0^t dt'\ \eta(t-t')\dot{q}(t')=F(t), \tag{3.1}$$

where q is the displacement in the bond length, $F(t)$ is the random force along the bond, and $\tilde{\omega}$ can be determined by the mean square displacement $\tilde{\omega}^{-2}=[\beta m\langle q^2\rangle]$. Using projection operator techniques, one can explicitly derive the expressions for the dynamic friction $\eta(t)$, the random force $F(t)$, and the second fluctuation dissipation theorem which relates the two. However, the formal definitions provide little help in evaluating these quantities. It is thus necessary to obtain the dynamical friction kernel by some other means. An often used approximation is to set the dynamical friction kernel equal to the autocorrelation function of the fluctuating force exerted on the rigid bond by the bath degrees of freedom. The rigid bond approximation has been shown to be the high frequency limit of true dynamical friction coefficient.[16]

If the bond motion can be characterized by a high frequency oscillation, the dynamic friction kernel is equivalent to that evaluated for a rigid bond fixed at the average position of the bond coordinate.[16] Then, the second dissipation theorem yields a simple prescription for the friction, i.e.,

$$\eta(t)=\beta\langle\delta F(t)\,\delta F(0)\rangle, \tag{3.2}$$

where the random force fluctuation $\delta F(t)$ is evaluated with the bond frozen at its equilibrium length. The explicit relation between the force fluctuations and the dynamic friction cannot be derived in general except if the nonlinear bond coordinate is bilinearly coupled to a harmonic bath, i.e.,

$$V=V_{\mathrm{eq}}(q)+\sum_{i=1}^{N}\omega_i^2\left(x_i-\frac{c_i}{\omega_i^2}\,q\right)^2, \tag{3.3}$$

where $V_{\mathrm{eq}}(q)$ is the potential of mean force along q, x_i is the ith Gaussian bath normal mode, and c_i is the coupling strength. It was shown by Zwanzig[4] that the elimination of the bath modes from the equations of motion for the above potential yields the GLE. The dynamical friction coefficient is then identified as

$$\eta(t)=\sum_{i=1}^{N}\frac{c_i^2}{\omega_i^2}\cos(\omega_i t)=\frac{2}{\pi}\int_0^\infty d\omega\ \frac{J(\omega)}{\omega}\cos(\omega t), \tag{3.4}$$

where $J(\omega)$ is the spectral density, defined in the discrete limit by

$$J(\omega)=\frac{\pi}{2}\sum_{i=1}^{N}\frac{c_i^2}{\omega_i}\,\delta(\omega-\omega_i). \tag{3.5}$$

The random force can be explicitly expressed in terms of the initial conditions of the bath variables. Therefore, under the

assumption that the initial bath distribution in phase space is in thermal equilibrium in the presence of the system, one can readily show that

$$\eta(t)=\beta\langle F(t)F(0)\rangle, \tag{3.6}$$

where the equilibrium condition $\langle F\rangle=0$ is implied.

The introduction of the spectral density $J(\omega)$ makes it possible to pass from a discrete set of modes to a continuum spectrum, and hence to represent an arbitrary time dependent friction $\eta(t)$. The relation in Eq. (3.6) holds for a harmonic bath regardless of the anharmonic bond potential or the bond length. It is for this reason that the Gaussian bath is an attractive analytical model to study the solvent frictional effects on vibrational relaxation and activated reaction dynamics. In a real system, the asymptotic limit of the friction mentioned previously implies that the frequency of the oscillating bond must be much larger than the peak frequency of the solvent spectral density.

While the GLE is an appealing picture, questions remain whether the harmonic bath is suitable for describing realistic systems and, if so, how the spectral density can be calculated from first principles. The rigor of such a derivation relies on the quadratic nature of the bath and the linearity of the couplings. This situation may be best realized in the solid state where the bath modes can be well understood as the phonon excitations. In contrast, there is not such a *global* quadratic bath for liquids, a bath defined as being independent of the temperature and density. In liquids, however, one can appeal to the concept of an *effective* Gaussian bath—precisely the target of this paper!

In the previous section, it was proposed that the configuration space of liquids can be partitioned into different optimized metastable potential subspaces so that the short time liquid motion is described as effective harmonic thermal excitations in the inherent structure wells. The optimized structure and the effective thermal fluctuations can then be found in a self-consistent fashion by virtue of the general OQA theory. Furthermore, the dynamics of liquids can be separated into the effective harmonic oscillations in the potential wells and the transitions between the different wells. In this simplified picture, liquids can be described as a set of damped harmonic oscillators. Following the same line of reasoning, one can picture a solute bond in a solvent as being coupled to a damped harmonic bath consisting of exponentially decaying normal modes. In light of the present theoretical developments, the harmonic bath can be identified as a set of optimized normal modes in the OQA theory. The normal modes thus defined will depend on the particular liquid configuration from which the optimized configuration is mapped. Therefore, the actual modes and couplings not only depend on the nature of the solvent, but also on the mass, flexibility, and length of the bond.

In order to formalize the DNM picture of dynamical friction, a modification of the OQA equations is necessary: The ONM solutions will apply to *all* degrees of freedom except the bond variable. This introduces an extended OQA theory with one or several degrees of freedom constrained so the projection of the solvent modes will introduce linear couplings and thus identify the origin of the dynamic friction in the DNM picture. For the present purposes, the formulation will be confined to the specific situation of a nonrotational rigid bond. From the perspective of the OQA, a flexible bond would allow for an optimization of the bond frequency and Gaussian fluctuations of the bond variables, whereas the rigid bond imposes constraints on the OQA equations. It should be noted, however, that in the high frequency limit the matrix element corresponding to the bond length variable becomes decoupled from other elements in both the force constant and Gaussian width matrices, so it actually makes little difference whether the bond length is held fixed or allowed to oscillate. Furthermore, when the bond does not rotate, the variables corresponding to the bond rotation will be constrained in the optimization. Similarly, when the center of the bond does not move, the variables corresponding to the bond translational motion will be constrained.

For a rigid bond at rest, the OQA equation can be written under the imposed constraints as

$$\langle \boldsymbol{\nabla} V\rangle_q=0, \tag{3.7}$$

$$\langle \boldsymbol{\nabla}:\boldsymbol{\nabla} V\rangle_q=\mathbf{K}, \tag{3.8}$$

where the gradients are in Cartesian space and the symbol $\langle\cdots\rangle_q$ denotes a Gaussian average in the optimized solvent normal modes. In both cases, the bond degree of freedom is appropriately constrained. After performing the optimization to find the ONM's, the equation for the coupling constants is giving by

$$\langle \boldsymbol{\nabla}_i \boldsymbol{\nabla}_q V\rangle_q=c_i, \tag{3.9}$$

where the subscript "i" stands for the ith ONM mode and q stands for the bond variable. Now comes an important point: To calculate the dynamical bond friction in the DNM picture, the *same* exponentially decaying function $f(t)$ is used as for the *pure solvent*, giving

$$\eta(t)=\frac{2}{\pi}\int d\omega\,\frac{J_{\mathrm{ONM}}(\omega)}{\omega}\cos(\omega t)e^{-\lambda t}$$

$$=e^{-\lambda t}\sum_{i=1}^{N}\frac{c_i^2}{\omega_i^2}\cos(\omega_i t), \tag{3.10}$$

where λ is the decay parameter from the pure solvent self-diffusion constant [cf. Eq. (2.19)]. The effective DNM spectral density function for the friction should be broadened according to the convolution relation in Eq. (2.16), i.e.,

$$J_{\mathrm{DNM}}(\omega)=\frac{1}{\pi}\int d\omega'\,\frac{\lambda}{\lambda^2+(\omega-\omega')^2}\,J_{\mathrm{ONM}}(\omega'). \tag{3.11}$$

IV. APPLICATIONS

A. A simple example

To test the concepts proposed in this paper, numerical calculations were performed for a one-dimensional double well potential, given by

$$V(q)=-\tfrac{1}{2}q^2+cq^3+gq^4 \tag{4.1}$$

with the parameters $c=0.01$, $g=0.1$, $m=1.0$, and $\beta=5.0$. The barrier for this potential is located at the origin, separating the two asymmetric wells. Obviously, there are two sets

of OQA solutions corresponding to the left-hand side and the right-hand side of the barrier. However, as the temperature is increased or the barrier height is sufficiently decreased, the two solutions merge into a single quadratic well near the origin, indicating that the thermal excitations overwhelm the barrier. (In contrast, for a many-body potential there exists a complicated branching and merging of the multidimensional OQA solutions as the temperature changes.) For comparison, the instantaneous normal mode (INM) correlation function was also calculated for this simple example. Moreover, in order to demonstrate the importance of self-consistently adjusting the equilibrium position to the center of the thermal excitation along with the fluctuation frequency, the normal mode equation Eq. (2.7) was also solved at the quenched potential minimum without optimizing the equilibrium position via Eq. (2.6). The resulting quenched normal mode spectrum (QNM) reflects the infinitesimal vibrations corresponding to the minima of Stillinger and Weber's mechanical stable structures (i.e., at zero temperature). The correlation function $C_{\mathrm{QNM}}(t)$ resulting from the QNM spectrum was assumed to also incorporate the exponential damping function.

Monte Carlo importance sampling was employed to generate the instantaneous configurations and the normal mode analysis was applied at each independent configuration: The INM frequency was determined by the local curvature, while the ONM equilibrium position and frequencies were chosen from the two sets of OQA solutions depending on the instantaneous position, as was the QNM frequency. The frequencies were accumulated to yield the corresponding normal mode spectra. To predict the velocity autocorrelation function, an exponential decay function with $\lambda=0.1$ was employed in Eq. (2.17). For comparison, the TST barrier crossing rate for the double well was evaluated to be about 0.15, which is somewhat larger than the optimal decay rate. Considering that the TST rate in this simple well certainly overestimates the true barrier crossing rate, the choice of λ is consistent with the interpretation that the incoherence of the ONM's arises from the barrier crossings.

In Fig. 1, the velocity autocorrelation functions are plotted for the exact MD simulation results, for the DNM prediction, for the QNM prediction, and for the stable-mode INM prediction. Clearly, the DNM correlation function gives the best agreement with the MD result, the QNM correlation function is out of phase, while the INM correlation function dephases too quickly after the second period. It should be noted that in this example, as well as in the following two, the correlation functions calculated by the different methods (i.e., MD, DNM, INM, QNM) have all been normalized to give the same initial ($t=0$) value. Since the initial value of a correlation function can be calculated exactly from equilibrium properties through a Monte Carlo or MD simulation, any approximate theory can always be calibrated to give the exact zero-time value. The important comparison to make here is in the time dependence of the correlation functions. It should also be noted that damping could be included in the stable mode INM correlation function as in Ref. 10, but it would need to have a significant frequency dependence in order to bring the INM result into better agreement with the exact one. That is, a simple exponential or Gaussian damping function in the INM theory would just worsen the agreement between the exact and INM correlation functions since the stable mode INM function already decays much too rapidly in this case.

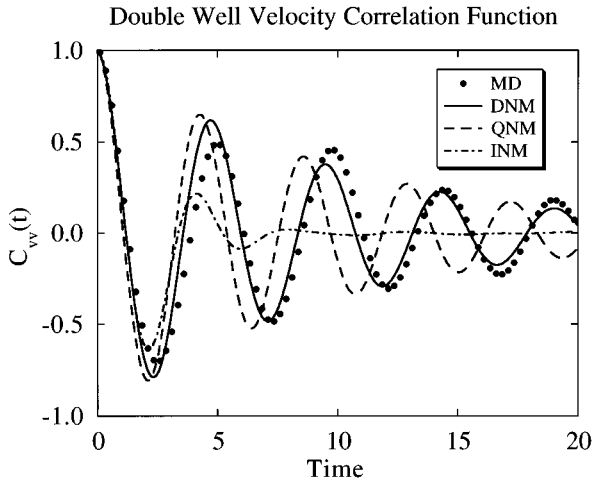

FIG. 1. A plot of the velocity autocorrelation function for the classical potential given by Eq. (4.1). The solid circles are the MD simulation results, the solid line is the DNM result, the dashed line is the QNM result, and the dash–dot line is the INM result with the unstable modes removed.

B. Velocity autocorrelation functions in liquids

The DNM theory was next applied to a simple homogeneous liquid of particles interacting through a pairwise potential, given by

$$V(r_{ij})=r_{ij}^{-12}, \tag{4.2}$$

where all quantities such as mass, length, time, energy, and temperature are assumed to be unity. The numerical studies were performed at a temperature of 1.2 and a density of 0.84. After the system was relaxed to equilibrium, independent liquid configurations following every 1000 Monte Carlo moves were used for the optimization. Following the steps described in the text, liquid configurations were sampled, quenched, and optimized. The ONM distribution function was accumulated over 300 independent liquid configurations. For comparison, MD simulations were performed for the same system, with 10^4 trajectories being integrated to yield the velocity time correlation function.

It can be time consuming to solve the self-consistent OQA equations for a many-body system. Fortunately, the thermal fluctuation matrix $\mathbf{C}$ is a relatively small quantity for many cases. Such a narrow Gaussian width allows one to Taylor expand the OQA equations through leading order, giving

$$\boldsymbol{\nabla}:\boldsymbol{\nabla}V+\tfrac{1}{2}\boldsymbol{\nabla}:\boldsymbol{\nabla}(\boldsymbol{\nabla}:\boldsymbol{\nabla})V\mathbf{C}=\mathbf{K} \tag{4.3}$$

and

$$\boldsymbol{\nabla}V+\tfrac{1}{2}\boldsymbol{\nabla}(\boldsymbol{\nabla}:\boldsymbol{\nabla})V\mathbf{C}=\boldsymbol{\nabla}(\boldsymbol{\nabla}V)\cdot(\overline{\mathbf{q}}-\overline{\mathbf{q}}_c), \tag{4.4}$$

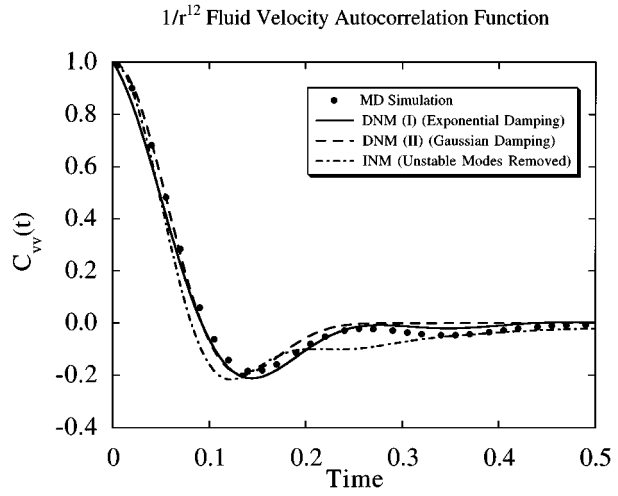

FIG. 2. A plot of the velocity autocorrelation function for a liquid with a pairwise potential given by Eq. (4.2). The solid circles are the MD simulation results, the solid line is the DNM (I) result for an exponential damping, the dashed line is the DNM (II) result for a Gaussian damping, and the dash–dot line is the INM result with the unstable modes removed.

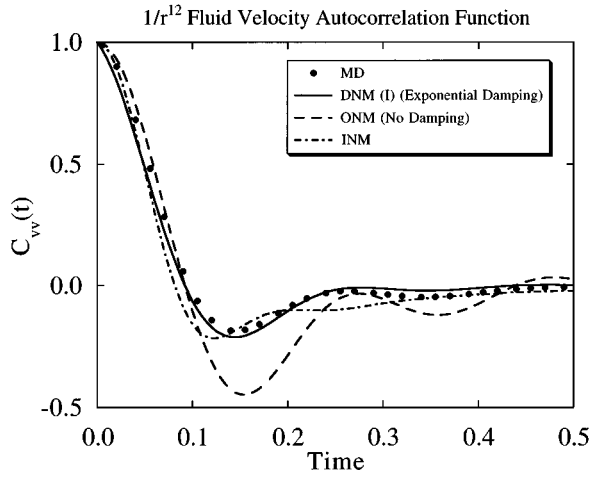

FIG. 3. A plot of the velocity autocorrelation function for a liquid with a pairwise potential given by Eq. (4.2). The solid circles are the MD simulation results, the solid line is the DNM (I) result for an exponential damping, the dashed line is the ONM result for no damping ($\lambda=0$), and the dash–dot line is the INM result with the unstable modes removed.

where all quantities are evaluated at the current optimized position $\overline{\mathbf{q}}_c$. The above equations can be solved iteratively until convergence is reached.

In Fig. 2, the normalized velocity correlation function calculated from the DNM analysis is plotted along with the MD simulation result and the stable-mode approximation for the INM correlation function.[19] An exponentially decay function with $\lambda=5.0$ is used for the DNM (I) correlation function, while a Gaussian decay function with the width factor κ determined from Eq. (2.22) is used for the DNM (II) correlation function. It can be seen from Fig. 2 that, as expected, both the INM and DNM (II) correlation functions agree with the MD simulation result at short times. At relatively long times, however, the INM correlation function becomes out of phase and the DNM (II) correlation function decays too rapidly. Overall, it is thus seen that the DNM (I) correlation function with the exponential damping function gives the best prediction of the liquid state dynamics. This example clearly demonstrates the feasibility and accuracy of the DNM theory for realistic systems. In Fig. 3, the exact and DNM (I) correlation functions are plotted along with the ONM correlation function having no damping factor (i.e., $\lambda=0$). The ''oscillation'' is correct in the latter case and there is some degree of dephasing due to the superposition of the different metastable well solutions, but the damping function is obviously required in order to obtain quantitative agreement with the MD result. Recall that the DNM theory explicitly *separates* the oscillations of the various inherent structures from the damping behavior due to the transitions between such structures.

As in the previous example, the accuracy of the DNM result illustrates the value of the variational determination of the ONMs. In particular, the phase of the correlation function oscillation is well reproduced in the DNM theory because the variational effective oscillator frequencies are chosen to model the *anharmonic* thermal fluctuations of the inherent structures. In contrast, the stable mode INM theory does not incorporate such a procedure since the stable INMs are determined from the instantaneous configurations of the liquid. The INM correlation function is therefore less accurate in reproducing the phase of the exact result, although a frequency-dependent damping function[10] might improve the accuracy of the INM theory (and, of course, the accuracy of the DNM theory as well). Unfortunately, the determination of such a function from first-principles or otherwise is not straightforward.

C. Dynamical friction on solute bonds

In this example, the system was the same as the liquid described in the previous subsection except that two of the atoms are not allowed to move. As was outlined in Sec. III, the solute molecule was rigid and held fixed with a separation of unit length. The solvent–solvent and solute–solvent site–site interactions were again given by the repulsive $1/r^{12}$ potential. To solve the self-consistent OQA equations, the Gaussian average was expanded through second-order and the solution was found iteratively. The details are very similar to those described in Sec. IV B. In the presence of the rigid solute, however, the solvent spectrum was modified accordingly due to the presence of the solute. In particular, the three translational invariants were broken, which correspond to three nonzero frequency normal modes. The dynamical friction on the bond in the DNM theory was then given by Eq. (3.4) with the exponential decay function and decay constant taken from the pure liquid described in Sec. IV B.

In the exact MD calculation, the solvent force parallel to the rigid bond direction $\hat{r}_{12}$ was projected out at each time step, giving

$$F(t)=\tfrac{1}{2}(\mathbf{F}_1(t)-\mathbf{F}_2(t))\cdot\hat{r}_{12}, \tag{4.5}$$

where $\mathbf{F}_i(t)$ is the force on atom i at time t.[16] The factor of 1/2 arises because the mass associated with the coordinate is

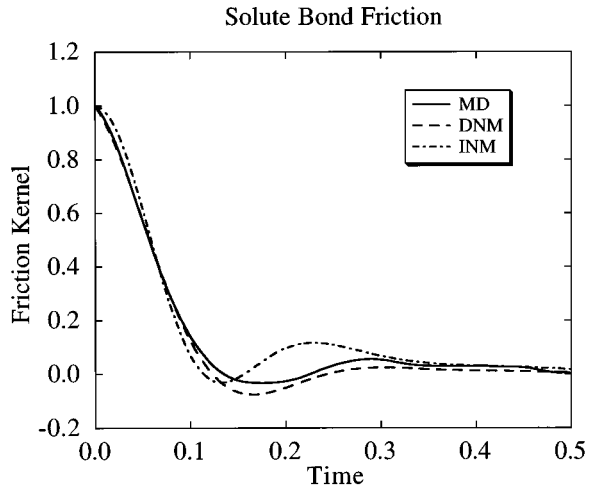

FIG. 4. A plot of the friction kernel for a rigid solute bond as described in Sec. IV C. The solid line is the MD result, the dashed line is the DNM prediction with the exponential damping parameter determined from the pure solvent, and the dash–dot line is the INM result with the unstable modes removed.

the reduced mass of the diatomic bond. The force autocorrelation function was then averaged over MD trajectories to give the dynamical friction kernel $\eta(t)$ of Eq. (3.6).

In Fig. 4, the dynamical friction kernels are shown as calculated from the DNM analysis with the damping parameter taken from the pure solvent, the INM stable mode approximation, and the MD simulation. All curves are normalized to be unity at $t=0$. Again, good agreement between the DNM and exact friction kernels is obtained, confirming that the DNM model can be an accurate approach for the calculation of dynamic friction on solute bonds. The stable mode INM approach is again less accurate in this example, perhaps requiring some kind of frequency-dependent damping function[10] to improve its agreement with the exact result.

V. CONCLUDING REMARKS

In this paper, a rigorous definition of the inherent liquid state structures and their metastable normal modes of vibration was developed in order to calculate liquid state correlation functions. From this perspective, equilibrium and transport properties can be studied in a systematic fashion. Though the exponential decay assumption for the optimized normal modes awaits a rigorous derivation, the intuitive picture of the damped oscillators is a compelling one which seems consistent with the linear regression hypothesis. Furthermore, the damping factor from the DNM solution for the pure solvent can be used along with the OQA theory to predict the friction on solute motions, thus providing a microscopic theory for the GLE friction kernel.

The OQA and DNM equations can be applied to a wide range of problems. As an example, the activated barrier crossing problem in condensed phases can be treated as an effective multidimensional quadratic system coupled to an unstable degree of freedom so that the standard TST approach can be used.[13,32] The Gaussian bath, the unstable mode, and the linear couplings can be solved from the extended ONM equations with the unstable coordinate constrained at the barrier top. This procedure leads to a Kramers–Grote–Hynes type rate constant,[32–34] but it incorporates in a self-consistent fashion the anharmonicity in the vicinity of the barrier, the nonlinearity of the bath, and the nonlinear couplings between the bath and the reactive coordinate. This theory can also be extended to the quantum mechanical limit, improving upon a result derived previously by one of us.[35] These and other applications of the present theory will be the subject of future publications.

ACKNOWLEDGMENTS

This research was supported by the National Science Foundation (CHE-9158079 and CHE-9410608) and the Office of Naval Research. G.A.V. is a recipient of a National Science Foundation Presidential Young Investigator Award, a David and Lucile Packard Fellowship in Science and Engineering, an Alfred P. Sloan Foundation Research Fellowship, and a Camille Dreyfus Teacher–Scholar Award.

APPENDIX A: QUANTUM DAMPED NORMAL MODE THEORY OF LIQUIDS

In the quantum mechanical limit, the OQA equations are written as[11]

$$\langle \nabla V(\overline{\mathbf{q}}+\tilde{\mathbf{q}})\rangle_{\mathbf{C}}=0, \tag{A1}$$

$$\langle \nabla:\nabla V(\overline{\mathbf{q}}+\tilde{\mathbf{q}})\rangle_{\mathbf{C}}=\mathbf{K}, \tag{A2}$$

where $\mathbf{K}$ is the optimized effective force constant matrix and where ∇ is the partial derivative vector $\nabla_i=\partial/\partial q_i$. The notation $\langle\cdots\rangle_{\mathbf{C}}$ where denotes a multidimensional Gaussian average centered at $\overline{\mathbf{q}}$, i.e.,

$$\langle V(\overline{\mathbf{q}}+\tilde{\mathbf{q}})\rangle_{\mathbf{C}}=\frac{1}{\sqrt{\det[2\pi\mathbf{C}]}}\int d\tilde{\mathbf{q}}\; V(\overline{\mathbf{q}}+\tilde{\mathbf{q}}) \times\exp[-\tilde{\mathbf{q}}\cdot\mathbf{C}^{-1}\cdot\tilde{\mathbf{q}}/2]. \tag{A3}$$

The Gaussian width factor matrix $\mathbf{C}$, in this case, can be formally expressed as

$$\mathbf{C}=\sum_{n=-\infty}^{\infty}[\beta\mathbf{m}\Omega_n^2+\beta\mathbf{K}]^{-1}, \tag{A4}$$

where $\mathbf{m}$ is the $3N$-dimensional mass matrix and $\Omega_n=2\pi n/\hbar\beta$. A unitary matrix $\mathbf{U}$ can be found to diagonalize the mass-scaled force constant matrix $\overline{\mathbf{K}}$, giving the quantum ONM frequencies

$$\mathbf{U}^{\dagger}\overline{\mathbf{K}}\mathbf{U}=[\mathbf{I}\cdot\overline{\omega^2}], \tag{A5}$$

where $\{\overline{\omega_i}\}$ is the set of the eigenfrequencies and $[\mathbf{I}\cdot\overline{\omega^2}]$ denotes a diagonal matrix with the ith diagonal element given by $\overline{\omega_i^2}$. The Gaussian width factor matrix in Eq. (A4) can be determined from the relation

$$\mathbf{C}=\overline{\mathbf{U}}[\mathbf{I}\cdot\overline{\alpha}]\overline{\mathbf{U}}^{\dagger}, \tag{A6}$$

where $\overline{\mathbf{U}}=\mathbf{m}^{-1/2}\mathbf{U}$ and the individual elements of the normal mode thermal width vector are given by

$$\overline{\alpha_i}=\frac{1}{\beta\overline{\omega_i^2}}\left\{\frac{(\hbar\beta\overline{\omega_i}/2)}{\tanh(\hbar\beta\overline{\omega_i}/2)}\right\}. \tag{A7}$$

Thus the set of optimized frequencies $\{\overline{\omega}\}$ and average positions $\{\overline{q}\}$ are variationally obtained as the self-consistent solution to the transcendental matrix Eqs. (A1) and (A2) in N-dimensional space.

One can next define a quantum ONM spectrum, giving

$$D_{\mathrm{ONM}}(\omega)=\frac{1}{3N}\sum_{i=1}^{3N}\langle\delta[\omega-\overline{\omega_i}(\mathbf{q}_0)]\rangle_{\mathbf{q}_0}, \tag{A8}$$

where $\overline{\omega_i}(\mathbf{q}_0)$ are the set of eigensolutions to Eq. (A5) for the region $R(l)$ mapped from an instantaneous liquid configuration $\mathbf{q}_0$. Following the DNM prescription, the quantum velocity correlation function for a simple atomic fluid is given by

$$C_{\mathrm{DNM}}(t)=\frac{1}{m\beta}\int d\omega\; D_{\mathrm{ONM}}(\omega)f_Q(\omega)\cos(\omega t)e^{-\lambda t}, \tag{A9}$$

where the quantum mode-weighting factor is given by

$$f_Q(\omega)=\frac{(\hbar\beta\omega/2)}{\tanh(\hbar\beta\omega/2)}. \tag{A10}$$

It should be noted that the quantum generalization of the DNM theory is particularly significant because information on quantum dynamics is very difficult to obtain for many-body systems using direct computer simulation techniques (as opposed to the classical case).

[1] M. Born and K. Huang, *Dynamical Theory of Crystal Lattices* (Clarendon, Oxford, 1955).
[2] C. Kittel, *Quantum Theory of Solids* (Wiley, New York, 1963).
[3] B. J. Berne and R. Pecora, *Dynamic Light Scattering* (Wiley-Interscience, New York, 1976).
[4] R. Zwanzig, J. Stat. Phys. **9**, 215 (1973).
[5] F. H. Stillinger and T. A. Weber, Phys. Rev. A **25**, 978 (1982).
[6] F. H. Stillinger and T. A. Weber, J. Chem. Phys. **80**, 4434 (1984).
[7] F. H. Stillinger and T. A. Weber, J. Chem. Phys. **81**, 5089 (1984).
[8] R. Zwanzig, J. Chem. Phys. **79**, 4507 (1983).
[9] B. Madan, G. Seeley, and T. Keyes, J. Chem. Phys. **92**, 7565 (1990).
[10] B. Madan, G. Seeley, and T. Keyes, J. Chem. Phys. **94**, 6762 (1991).
[11] J. Cao and G. A. Voth, J. Chem. Phys. **102**, 3337 (1995).
[12] R. Kubo, N. Toda, and N. Hashitsume, *Statistical Physics II* (Springer, Berlin, 1985).
[13] P. Hanggi, P. Talkner, and M. Borkovec, Rev. Mod. Phys. **62**, 250 (1990).
[14] R. Zwanzig and M. Bixon, Phys. Rev. A **2**, 2005 (1970).
[15] B. J. Berne, J. Chem. Phys. **56**, 2164 (1972).
[16] B. J. Berne, M. E. Tuckerman, J. E. Straub, and A. L. R. Bug, J. Chem. Phys. **93**, 5084 (1990).
[17] G. Seeley and T. Keyes, J. Chem. Phys. **91**, 5581 (1989).
[18] B. Xu and R. M. Stratt, J. Chem. Phys. **92**, 1923 (1990).
[19] M. Buchner, B. M. Ladanyi, and R. M. Stratt, J. Chem. Phys. **97**, 8522 (1992).
[20] G. Seeley, T. Keyes, and B. Madan, J. Phys. Chem. **96**, 4074 (1992).
[21] Y. Wan and R. Stratt, J. Chem. Phys. **100**, 5123 (1994).
[22] T. M. Wu and R. F. Loring, J. Chem. Phys. **97**, 8568 (1992).
[23] T. M. Wu and R. F. Loring, J. Chem. Phys. **99**, 8936 (1993).
[24] T. Keyes, J. Chem. Phys. **101**, 5081 (1994).
[25] J. Cao and G. A. Voth, J. Chem. Phys. **101**, 6184 (1994).
[26] M. Cho, G. R. Fleming, S. Saito, I. Ohmine, and R. M. Stratt, J. Chem. Phys. **100**, 6672 (1994).
[27] B. M. Ladanyi and R. M. Stratt, J. Phys. Chem. **99**, 2502 (1995).
[28] P. F. Choquard, *The Anharmonic Crystals* (Benjamin, New York, 1967).
[29] V. Samathiyakanit and H. R. Glyde, J. Phys. C **6**, 1166 (1973).
[30] J. P. Stoessel and P. G. Wolynes, J. Chem. Phys. **80**, 4502 (1984), this paper contains an application of the self-consistent phonon idea to an amorphous material (i.e., the hard sphere glass).
[31] A TST-like approach has been developed in Ref. 24 within the context of the INM theory to describe liquid state self-diffusion. This approach assumes a relationship exists between the barrier height distribution and the unstable INM distribution. Since there are no unstable modes in the ONM spectrum, a rather different approach would be required to estimate the barrier height distribution between the inherent structures in the DNM theory. Nevertheless, the spirit of the two approaches would be the same.
[32] E. Pollak, J. Chem. Phys. **85**, 865 (1986).
[33] H. A. Kramers, Physica **7**, 284 (1940).
[34] R. F. Grote and J. T. Hynes, J. Chem. Phys. **73**, 2715 (1980).
[35] G. A. Voth, Chem. Phys. Lett. **170**, 289 (1990).